Organic & Biomolecular Chemistry

PAPER

View Article Online
View Journal | View Issue

Open Access Article. Published on 12 March 2019. Downloaded on 2/11/2026 1:35:32 PM.
This article is licensed under a Creative Commons Attribution-NonCommercial 3.0 Unported Licence.

Check for updates

Cite this: *Org. Biomol. Chem.*, 2019, **17**, 3529

On the reactivity of anodically generated trifluoromethyl radicals toward aryl alkynes in organic/aqueous media†

Wolfgang Jud,[a,b] C. Oliver Kappe *[a,b] and David Cantillo *[a,b]

Received 23rd February 2019,
Accepted 12th March 2019

DOI: 10.1039/c9ob00456d

rsc.li/obc

An in-depth study of the reaction of electrochemically generated trifluoromethyl radicals with aryl alkynes in the presence of water is presented. The radicals are readily generated by anodic oxidation of sodium triflinate, an inexpensive and readily available CF_3 source, with concomitant reduction of water. Two competitive pathways, *i.e.* aryl trifluoromethylation *vs.* oxytrifluoromethylation of the alkyne, which ultimately lead to the generation of α-trifluoromethyl ketones, have been observed. The influence of several reaction parameters on the reaction selectivity, including solvent effects, electrode materials and substitution patterns on the aromatic ring of the substrate, has been investigated. A mechanistic rationale for the generation α-trifluoromethyl ketones based on cyclic voltammetry data and radical trapping experiments is also presented. DFT calculations carried out at the M06-2X/6-311+G(d,p) level on the two competing pathways account for the observed selectivity.

Introduction

Incorporation of perfluoroalkyl moieties into organic molecules typically enhances some of their biological properties such as metabolic stability, lipophilicity and bioavailability,[1] and hence represents an important type of modification in the production of agrochemicals, materials and pharmaceuticals (Fig. 1).[2] Over the past two decades, a plethora of synthetic methods for the generation of C–C bonds between perfluoroalkyl groups and organic scaffolds have been reported.[3] In particular, research on the introduction of trifluoromethyl groups (CF_3) has gained significant attention.[4] To this end, a variety of different trifluoromethyl donors have been developed, ranging from simple and inexpensive compounds, such as triflyl chloride,[5] trifluoroiodomethane,[6] trifluoromethyltrialkylsilane[7] and sodium triflinate,[8] to more complex and expensive chemicals like Umemoto's or Togni's reagents.[9] In particular, the generation of α-trifluoromethyl ketones, which may serve as versatile building blocks for a diverse set of CF_3-containing molecules, has been subjected to intense research and is considered to be an especially challenging task.[10] Common synthetic protocols involve electrophilic or radical trifluoromethylations of silyl enol ethers,[10–12] or enamines,[13] which are generated as reactive intermediates from the parent ketone. Ideally, isolation of these intermediates is avoided, affording a one-pot, two-step procedure.[12] Alternatively, α-trifluoromethyl ketones can be obtained by direct radical trifluoromethylation of alkenes[14] or alkynes[15] in the presence of an oxidizing agent (*e.g.* molecular oxygen) or a hydroxyl source, respectively.

Radical trifluoromethylations are typically promoted by chemical oxidation of a CF_3 source or photochemical methods (*e.g.* photoredox catalysis).[4] Generation of CF_3 radicals can also

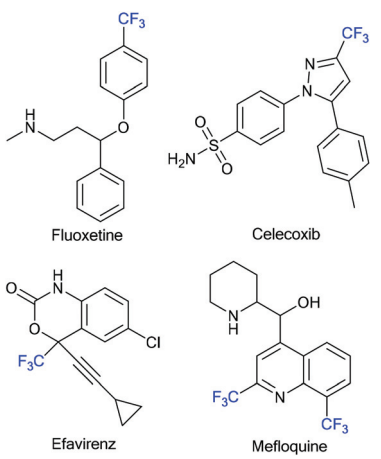

Fig. 1 Examples of CF_3-containing active pharmaceutical ingredients.

[a]*Institute of Chemistry, University of Graz, NAWI Graz, Heinrichstrasse 28, 8010 Graz, Austria. E-mail: oliver.kappe@uni-graz.at, david.cantillo@uni-graz.at*
[b]*Center for Continuous Flow Synthesis and Processing (CC FLOW), Research Center Pharmaceutical Engineering GmbH (RCPE), Inffeldgasse 13, 8010 Graz, Austria*

†Electronic supplementary information (ESI) available: Supplementary figures and tables, copies of NMR spectra and Cartesian coordinates and energies of all calculated structures. See DOI: 10.1039/c9ob00456d

Open Access Article. Published on 12 March 2019. Downloaded on 2/11/2026 1:35:32 PM.
This article is licensed under a Creative Commons Attribution-NonCommercial 3.0 Unported Licence.

be achieved by electrochemical methods, enabling the aforementioned redox process without the need for metal- or photocatalysts or stoichiometric amounts of hazardous oxidizing or reducing agents, giving rise to highly sustainable processes.[16] In fact, owing to the "inherently green" character of electroorganic synthesis,[17] this technology has seen a considerable resurgence over the past few years. Generation of CF_3 radicals by anodic oxidation of several CF_3 sources, including CF_3COOH,[18] CF_3SO_2Na,[19] or $(CF_3SO_2)_2Zn$,[20] and its application in the trifluoromethylation of arenes and alkenes have been reported. Recently, we have developed a novel route for the oxytrifluoromethylation of alkenes, enabled by the electrochemical oxidation of CF_3SO_2Na in the presence of water.[21]

Herein, the reactivity of anodically generated CF_3 radicals in organic/aqueous media is extended to more challenging aryl alkyne substrates. A rather similar nucleophilic character of the alkyne and the aromatic moiety results in a competition between two reaction pathways: oxytrifluoromethylation of the alkyne, which leads to the corresponding α-trifluoromethyl ketone after tautomerization of the ensuing enol, and arene trifluoromethylation (Fig. 2). In an attempt to harness reaction selectivity, the effect of several reaction parameters on product distribution has been carefully studied. Formation of α-trifluoromethyl ketones was favored in most cases, although mixtures with trifluoromethyl-aryl products were always observed. DFT calculations at the M06-2X/6-311+G(d,p) level on the two competing pathways have been carried out to explain the observed selectivity.

Results and discussion

Aryl *vs.* alkyne trifluoromethylation: effect of the solvent composition and electrode materials on reaction selectivity

Our investigation was carried out using 4-*tert*-butylphenylacetylene (**1a**) as a model aryl alkyne. All experiments were carried out in a standardized electrochemical reactor (IKA ElectraSyn) at constant current under a nitrogen atmosphere. An initial set of experiments was performed to evaluate the influence of the organic solvent, electrode material and electrolyte on the reaction outcome. All experiments were carried out on a 0.5 mmol scale, using a 0.2 M concentration for the alkyne and 1.2 equiv. CF_3SO_2Na. A constant current of 30 mA and a total charge of 2.2 F mol^{-1} (10% excess over the theoretical charge required) were applied. Notably, good to excellent conversions were obtained in all cases and, as anticipated, mixtures of the α-trifluoromethyl ketone **2a** and trifluoromethyl-aryl derivatives **3a–4a** were detected by GC analysis. Thus, in addition to the expected trifluoromethylaryl alkyne **3a**, aryl trifluoromethylation of the α-trifluoromethyl ketone **2a** (compound **4a**) was also observed. Formation of **4a** is expected to take place in the later stage of the reaction, when high concentrations of **2a** are present in the mixture (*vide infra*). Minor amounts (<5%) of trifluoromethylsulfonylated aromatics were also observed in some cases (for a GC-FID chromatogram of an example of the crude reaction, see Fig. S1 in the ESI†).

Using acetone as the solvent, a series of anode/cathode material combinations were evaluated (Table 1, entries 1–4). While maintaining graphite as the anode, altering the cathode material (graphite, Pt, Ni, stainless steel) only had a minor influence on the reaction outcome, with **2a** being formed with highest selectivity (Table 1, entries 1–4). In contrast, complex mixtures of products were obtained with both Pt and RVC as anodes (Table 1, entries 5 and 6). This could be attributed to lower overpotentials for some undesired oxidations on Pt, or the fact that its surface may be catalytically active for such side-reactions, and a poor mixing of the reaction mixture within the pores in the case of the RVC material.

Next, a series of solvents covering a wide range of dielectric constants were screened (ε = 35.7 for MeCN and ε = 7.5 and 7.0 for MeTHF and THF, respectively). The solvent choice may influence both the electrolysis efficiency, as the maximum amount of current that can be passed to the reagent solution while keeping the voltage in a 3–4 V range depends on the dielectric constant of the solvent, and the selectivity of the reaction itself. Best conversions were typically obtained in acetone. In addition, acetone favored the formation of **2a**, with a selectivity of up to 67% (Table 1, entry 3). Notably, the selectivity could be inverted in THF and MeTHF (entries 7 and 8). A selectivity of 65% toward aryl trifluoromethylation was observed using MeTHF as the solvent (entry 8), although the reaction conversion was significantly lower than that for acetone. Using MeOH as the solvent, an α-trifluoromethyl methyl-enol ether was formed as a product with 48% selectivity, resulting from methoxide acting as a nucleophile instead of water (Table 1, entry 10) (see Fig. S2 in the ESI†). Although full conversion was obtained in DCM, *ca.* 30% of an undesired, unidentified side-product was detected by GC. The type of electrolyte used had little influence on the product distribution (Table 1, entries 12 and 13). An additional experiment under potentiostatic conditions (constant voltage of 4 V) showed no noticeable difference to the reaction at constant current (Table 1, entry 14 *vs.* entry 4). As expected, the reaction did not

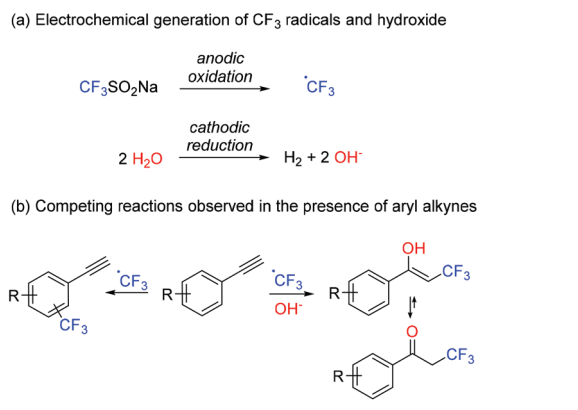

Fig. 2 (a) Generation of CF_3 radicals by anodic oxidation of sodium triflinate with concomitant reduction of water and (b) competition between oxytrifluoromethylation and aryl trifluoromethylation in the presence of aryl alkynes.

 This journal is © The Royal Society of Chemistry 2019

Open Access Article. Published on 12 March 2019. Downloaded on 2/11/2026 1:35:32 PM.
This article is licensed under a Creative Commons Attribution-NonCommercial 3.0 Unported Licence.

Table 1 Influence of the electrode type, solvent and electrolyte on the outcome of the reaction of **1a** with CF_3SO_2Na under constant current electrolysis in organic/aqueous media[a]

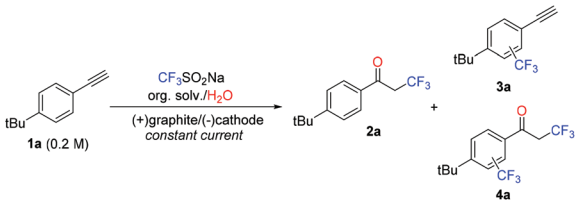

Entry	Solvent[b]	Anode	Cathode	Electrolyte	Conv.[c] [%]	**2a**[c] [%]	**3a–4a**[c] [%]
1	Acetone	Graphite	Graphite	Et_4NBF_4	92	63	37
2	Acetone	Graphite	Pt	Et_4NBF_4	93	61	25
3	Acetone	Graphite	Ni	Et_4NBF_4	94	67	33
4	Acetone	Graphite	SS	Et_4NBF_4	90	63	37
5	Acetone	RVC[d]	SS	Et_4NBF_4	99	10	20
6	Acetone	Pt	Pt	Et_4NBF_4	85	22	21
7	THF	Graphite	SS	Et_4NBF_4	51	23	53
8	MeTHF	Graphite	SS	Et_4NBF_4	24	35	65
9	MeCN	Graphite	SS	Et_4NBF_4	62	44	43
10	MeOH	Graphite	SS	Et_4NBF_4	73	48[e]	52[f]
11	CH_2Cl_2	Graphite	SS	Et_4NBF_4	99	41	31
12	Acetone	Graphite	SS	Bu_4NBF_4	85	62	34
13	Acetone	Graphite	SS	$LiClO_4$	85	46	37
14[g]	Acetone	Graphite	SS	Et_4NBF_4	97	64	36
15[h]	Acetone	Graphite	SS	Et_4NBF_4	<LOD	<LOD	<LOD

[a] Conditions: 0.5 mmol scale, 1.2 equiv. CF_3SO_2Na, 0.1 M electrolyte, 2.2 F mol^{-1}, constant current (30 mA) electrolysis under a N_2 atmosphere, 400 rpm stirring, and IKA ElectraSyn 2.0 reactor. [b] 20 : 1 mixture of the solvent and water. [c] Determined by GC-FID peak area integration. [d] Reticulated vitreous carbon. [e] Selectivity calculated for α-trifluoromethyl methyl-enol ether (see the ESI for details). [f] Selectivity calculated for trifluoromethylation of the substrate or enol ether on the aromatic ring. [g] Constant voltage (4 V) applied. [h] Without electricity.

proceed in the absence of electricity, proving that an electrochemical redox process was involved in the generation of the CF_3 radicals (Table 1, entry 15).

An additional set of reaction parameters, namely the amount of water and CF_3SO_2Na, temperature, concentration, current and total charge, was next investigated (Fig. 3). Conversion increased when low amounts of water were utilized (Fig. 3a). Notably, the **2a : 3a–4a** ratio decreased with increasing amounts of water, and the favored product was inverted when the amount of water increased from 47 to 97 equiv. The increase of temperature, substrate concentration, amount of CF_3SO_2Na and charge had positive effects on the reaction conversion, but a less important influence on the **2a : 3a–4a** product ratio (Fig. 3b–e). Low currents (Fig. 3f) favored higher **2a : 3a–4a** ratios, as well as higher substrate conversion. In most cases, α-trifluoromethyl ketone **2a** was the favored product of the reaction. As mentioned above, an excess of CF_3SO_2Na was required to achieve high conversions. ^{19}F-NMR monitoring of the reaction mixture revealed consumption of more than one equivalent of sodium triflinate at conversions below 90%. This effect could be ascribed to trapping of some of the CF_3 radicals by *e.g.* water and formation of volatile species.

Effect of substrate substituents. Reaction scope

To evaluate the functional group tolerance under the electrolysis conditions and assess their effect on the reaction selectivity, a diverse set of aryl alkynes was subjected to the electrochemical trifluoromethylation (Scheme 1). α-Trifluoromethyl ketones **2** were favored in most cases. For that reason, derivatives **2** were isolated and characterized. Yields for **2** and the trifluoromethyl-aryl adducts **3–4** were also determined by ^{19}F NMR for comparison. Since the reactions were carried out in acetone, minor amounts (<10%) of the acetone aldol condensation products were detected in some reaction mixtures, which were likely formed under the basic conditions generated during the reaction. These impurities could easily be removed by evaporation.

Aromatic alkynes bearing both electron withdrawing and electron donating substituents, as well as a heterocyclic aryl alkyne, were reacted with $NaSO_2CF_3$ under electrolytic conditions (see the Experimental section for details). Surprisingly, despite the presence of deactivating functional groups on the arene in substrates **1b** and **1f**, the ratio of products did not shift in favor of the α-trifluoromethyl ketone **2**. In contrast, during the reaction of the electron-rich 4-methoxyphenyl acetylene (**1e**), trifluoromethylation of the ring was clearly favored (Scheme 1). The CF_3 radical addition reaction proved to be tolerant to steric effects, as both *para* methyl (**1h**) and *ortho* methyl (**1g**) phenylacetylene could be functionalized with similar yields. A non-terminal alkyne (**1j**) was also successfully derivatized under the standard reactions conditions. Notably, even the oxidatively labile substrate **1c** was converted into the α-trifluoromethyl ketone **2c** in modest yield. Isolation of pure

Open Access Article. Published on 12 March 2019. Downloaded on 2/11/2026 1:35:32 PM.
This article is licensed under a Creative Commons Attribution-NonCommercial 3.0 Unported Licence.

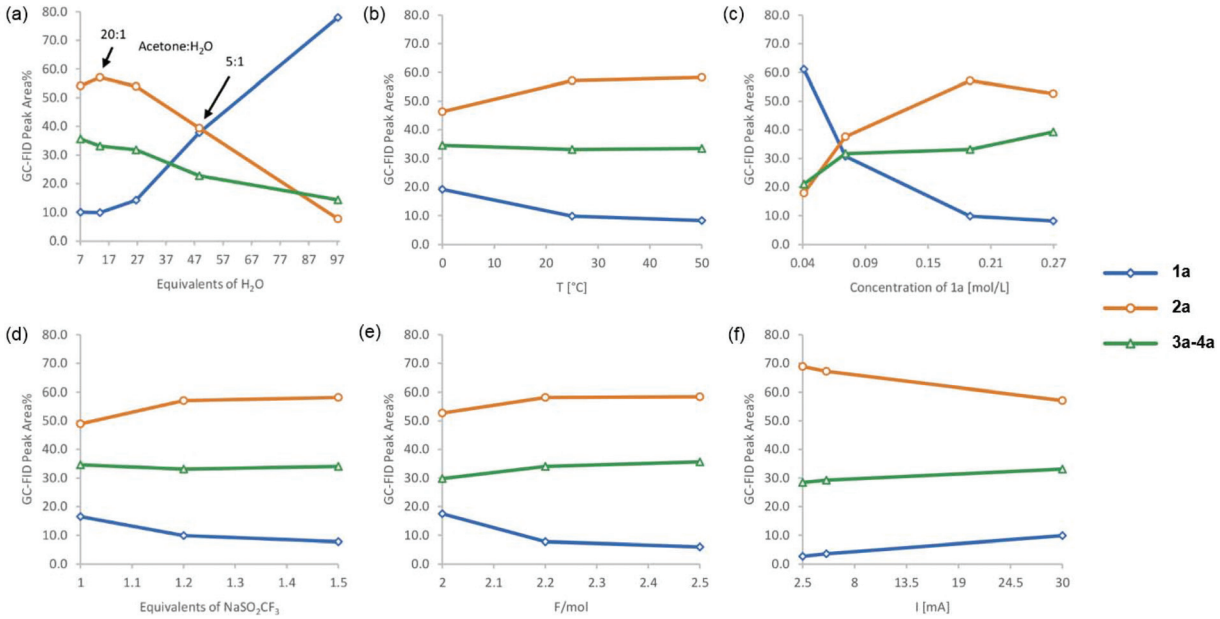

Fig. 3 Influence of the amount of water (a), temperature (b), concentration (c), equivalents of CF_3SO_2Na (d), charge (e) and current (f) on the electrochemical transformation of **1a**. Typical conditions: 0.5 mmol substrate, 1.2 equiv. CF_3SO_2Na, acetone : H_2O 20 : 1 (v/v), 0.1 M Et_4NBF_4, 2.2 F mol^{-1}, constant current (30 mA), anode: graphite, cathode: stainless steel, and 2.625 mL reaction volume. For a more detailed representation, including the amounts of all side products, see Fig. S3 in the ESI†.

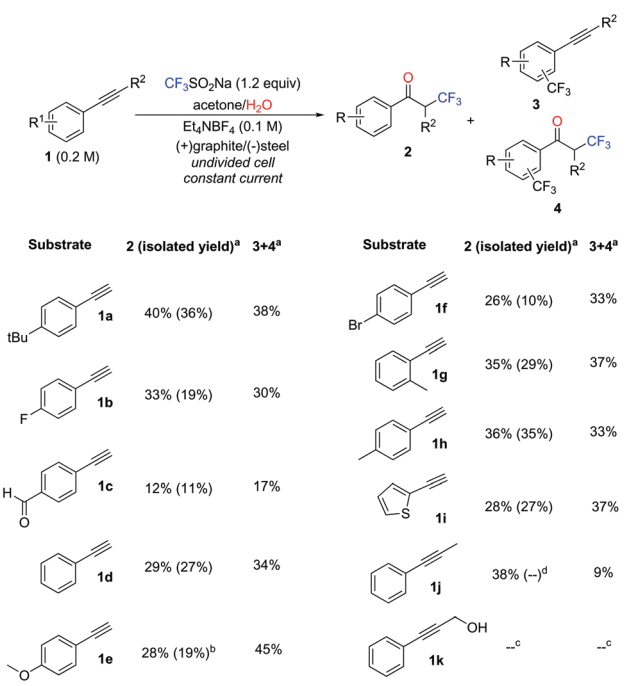

Scheme 1 Reaction scope for the electrochemical transformation of alkynes in the presence of $NaSO_2CF_3$. Conditions: 1.0 mmol substrate, 1.2 equiv. $NaSO_2CF_3$, acetone : H_2O 20 : 1 (v/v), 0.1 M Et_4NBF_4, 2.2 F mol^{-1}, constant current (15 mA), anode: graphite, cathode: stainless steel, and 5 mL reaction volume [a] Determined by ^{19}F-NMR. [b] Essay corrected; the isolated material (32%) contained **3e**. [c] See Scheme 2. [d] Ketone **2j** could not be separated from the side products by column chromatography.

α-trifluoromethyl ketones from the other reaction products was possible by simple column chromatography. Separation of **2e** from **3e** and **2j** from **3j** was problematic due to the very similar polarity of the products.

In an attempt to improve the reaction of oxidatively labile substances (*e.g.* **1c** and **1k**), three common oxidation mediators [triphenylamine, TEMPO and manganese(III) acetate dihydrate] were evaluated for the trifluoromethylation of these substrates as well as the model alkyne **1a**. Although a decrease of the current from 30 mA to 5 mA had a positive effect on the conversion of **1a** and **1c**, the presence of mediators did not significantly change the reaction outcome (see Table S1 in the ESI†). Notably, the reaction of **1k** did not afford the expected ketone **2**, but trifluoromethylacrylophenone **5** (Scheme 2). This compound is likely formed by intramolecular trapping of the carbocation intermediate **6** by the OH group (instead of water, which leads to the expected product **2**). The ensuing unstable oxetane **7** rearranges to compound **5**. Although **5** was observed

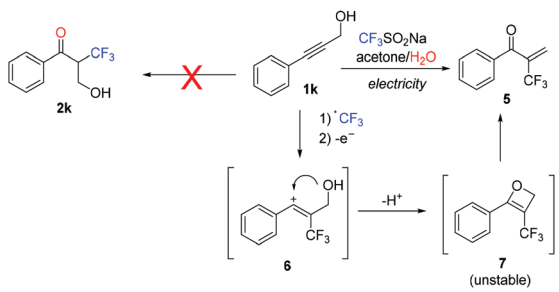

Scheme 2 Reaction outcome for alkyne **1j** utilizing the typical electrolysis conditions (Scheme 1).

 This journal is © The Royal Society of Chemistry 2019

Open Access Article. Published on 12 March 2019. Downloaded on 2/11/2026 1:35:32 PM.
This article is licensed under a Creative Commons Attribution-NonCommercial 3.0 Unported Licence.

in good yields (54%) by GC, its high reactivity did not allow its isolation in pure form (see Fig. S4 in the ESI†).

Proposed mechanism for the generation of α-trifluoromethyl ketones

Cyclic voltammograms of the starting materials (Fig. 4a) revealed that oxidation of sodium triflinate occurs at 1.1–1.3 V (*vs.* Ag/AgCl), and is followed by an irreversible reaction, while the model aryl alkyne substrate **1a** and even oxidatively labile alkynes require much higher oxidation potentials (2.2–2.5 V) (see Fig. 4a and S5 in the ESI† for other alkynes). Thus, oxidation at the anode should involve the CF_3 source with good selectivity.

Oxidation of triflinate is known to generate CF_3 radicals,[8,19] likely by decomposition of the initially formed CF_3SO_2 radical, as pointed out by the side products observed in the reaction (see Fig. S6 in the ESI†). To provide evidence for a radical reaction mechanism, we carried out a control experiment using the typical electrolysis conditions (Scheme 1) for the model substrate **1a** and using 1 equiv. of butylated hydroxytoluene (2,6-di-*tert*-butyl-4-methylphenol, BHT) as the additive. Cyclic voltammetry confirmed that BHT is oxidized at higher potential than CF_3SO_2Na, and therefore it is a suitable radical trapping agent for this reaction (see Fig. S5 in the ESI†). GC-MS analysis of the mixture after electrolysis revealed (see Fig. S7 in the ESI†) the presence of a large amount of unreacted **1a**, confirming that BHT quenched the reaction, as well as trifluoromethylated BHT and small amounts of α-trifluoromethyl ketones **2a** and **3a**. To our delight, compound **8** (Fig. 3b), corresponding to the trapping of a plausible trifluoromethylalkenyl radical, could also be detected by GC-MS analysis.

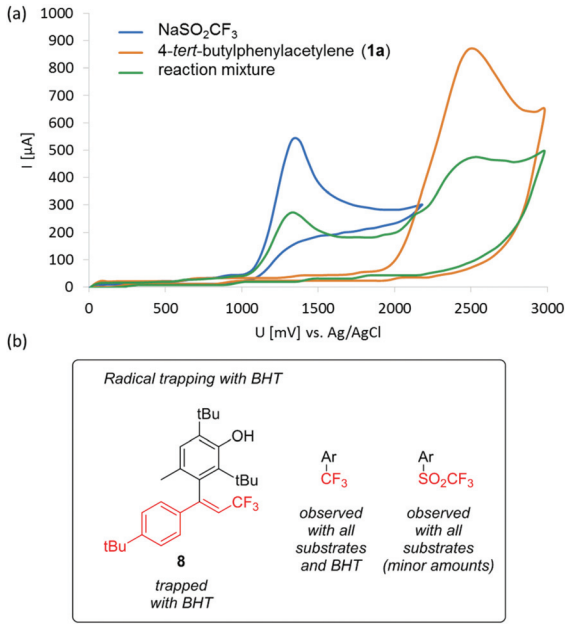

Fig. 4 (a) Cyclic voltammograms of CF_3SO_2Na, 4-*tert*-butylphenylacetylene (**1a**) and a typical reaction mixture (see the ESI† for details). (b) Species detected by GC-MS that point to the presence of the radical species highlighted in red.

Thus, the proposed mechanism for the formation of α-trifluoromethyl ketones (Fig. 5) starts with the anodic oxidation of the triflinate anion, producing a trifluoromethylsulfonyl radical which decomposes into a CF_3 radical and SO_2. Subsequently, the CF_3 radical adds to the triple bond of the substrate in an anti-Markovnikov fashion, giving rise to the secondary alkyl radical **9** stabilized by the adjacent aromatic ring. Further oxidation of **9** produces carbocation **10**. The carbocationic species is trapped by water or the hydroxide generated at the cathode, affording an enol ether **6**, which tautomerizes to the ketone **2**. The proposed mechanism represents an example of a paired electrochemical reaction: the hydroxide ions generated at the cathode during the electrolysis are also involved in the reaction, as one equivalent of hydroxide is incorporated into the final molecule.

Differential selectivity analysis and computational evaluation

As described above, reactions of aryl alkynes with electrochemically generated CF_3 radicals in the presence of water produced mixtures of α-trifluoromethyl ketones **2** and products derived from trifluoromethylation of the aromatic ring (**3a**–**4a**). This occurred under all reaction conditions evaluated (Table 1 and Fig. 2) and with all aryl alkynes tested (Scheme 1). Motivated by these somewhat surprising results–the reaction could not be directed to one of the two expected products, we decided to have a more detailed look into the reaction kinetics and assess the two competing pathways by DFT calculations, with the aim of providing an explanation to the observed product distribution.

HPLC monitoring of the model reaction (Fig. S8†) revealed the expected formation of compounds **2a** and **3a** from the initial reaction stage, and a gradual increase in the amount of

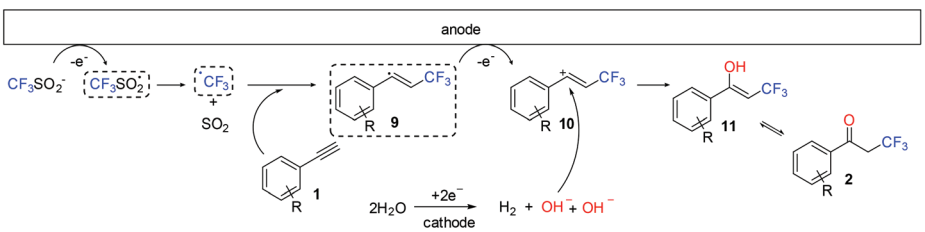

Fig. 5 Proposed reaction mechanism for the formation of α-trifluoromethyl ketones **2** from alkynes and electrochemically generated CF_3 radicals in the presence of water.

Open Access Article. Published on 12 March 2019. Downloaded on 2/11/2026 1:35:32 PM.
This article is licensed under a Creative Commons Attribution-NonCommercial 3.0 Unported Licence.

4a starting after 0.5 F mol^{-1}. This is due to the fact that **4a** is formed from **2a**. The reaction selectivity can be more clearly visualized by analyzing the corresponding differential selectivity plots (Fig. 6), which represent the relative amount of the reaction products at different reaction stages. Thus, the linear differential selectivity plot obtained for **2a** *vs.* **3a** (Fig. 6a) showed that the generation of the two compounds occurs simultaneously during the whole process, with a constant relative rate. The slope of the linear plot (*ca.* 0.32) indicated that the formation of **2a** is approximately 3 times faster than that of **3a**. Selectivity values for **2a** did not match this relative rate (*cf.* Table 1) due to the formation of other side products (*e.g.* **4a**), which take place at later stages of the reaction as shown in Fig. 6b. Thus, the differential selectivity of **2a** *vs.* the sum of all trifluoromethyl-aryl products (**3a**, **4a** and minor amounts of trifluoromethylsulfonyl derivatives) has a curved concave shape, indicating that the rate of formation of trifluoromethyl arenes increases with respect to the formation of **2a** with the reaction progress. These results were expected, as the rate of formation of **4a** is proportional to the amount of **2a** in the reaction mixture.

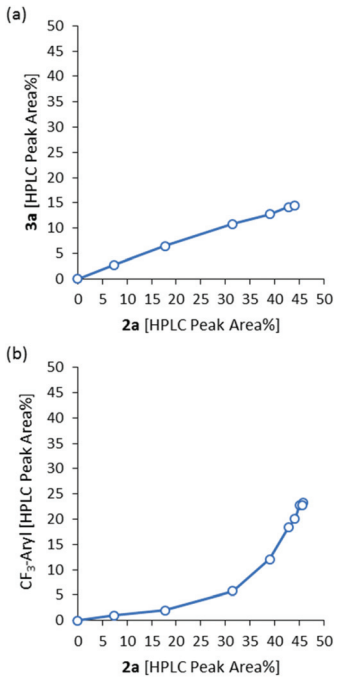

Fig. 6 Differential selectivity plots for the formation of **2a** *vs.* **3a** (a) and **2a** *vs.* aryl-trifluoromethyl species (b), obtained by HPLC monitoring of the reaction mixture.

The two reaction pathways, leading to the generation of compounds **2** and **3**, were then assessed by DFT calculations to ascertain the origin of the product distribution experimentally observed. Thus, the stationary points involved in the addition of the CF_3 radical to the alkyne and aromatic ring were modelled using the M06-2X functional[22] and the 6-311+G(d,p) basis set. All calculations incorporated solvent effects with the SMD model,[23] both for geometry optimization and frequency analyses, using acetone as the solvent. To reduce the computational cost of the calculations, the reaction of phenyl acetylene (**1d**) was selected as a model. The results were compared with the reaction of the trifluoromethyl radical with styrene (**1d′**) (Fig. 7a), which in previous studies had shown a clear preference for the radical addition to the olefin over the addition to the aromatic ring.[21] While the reaction of the CF_3 radical with the alkyne and the alkene was simply modelled for the C-2 addition, matching experimental observations, the radical addition to the aromatic ring was calculated for the *ortho*-, *meta*-, and *para*-positions. In the case of styrene, the two possible isomers for the *ortho*- and *meta*-addition of the CF_3 radical (depending on the alkene orientation) were taken into account. The energy of the most stable isomer is presented.

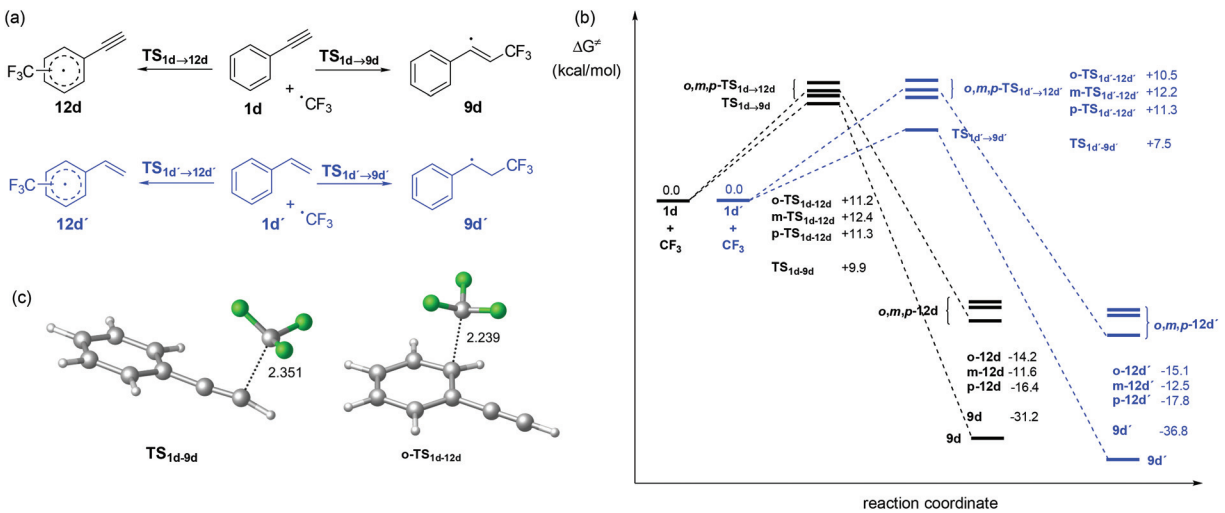

Fig. 7 (a) Computed radical additions to the aromatic ring and the alkyne (**1d**) or alkene (**1d′**); (b) energy profiles calculated at the M06-2X/6-311+G (d,p) level. The similar energy barriers obtained for the radical additions to the alkyne and arene of **1d** explain the mixtures of products observed experimentally; (c) structures of selected transition states.

 This journal is © The Royal Society of Chemistry 2019

Open Access Article. Published on 12 March 2019. Downloaded on 2/11/2026 1:35:32 PM.
This article is licensed under a Creative Commons Attribution-NonCommercial 3.0 Unported Licence.

The energy profile obtained for the reaction of phenyl acetylene (**1d**) with the CF_3 radical (Fig. 7b, black color) revealed analogous energy barriers for all possible radical addition pathways, being all within a range of *ca.* 2 kcal mol^{-1}. The difference in energy between the transition state for the radical addition to the triple bond ($\mathbf{TS_{1d-9d}}$) and the most favored of the arene additions ($\boldsymbol{o}$-$\mathbf{TS_{1d-12d}}$) was only 1.3 kcal mol^{-1}. Importantly, the similar energetics for the competing reactions satisfactorily explains the mixtures of products observed in all cases (*cf.* Table 1 and Fig. 2). As expected, the generation of adducts **9d** and **12d** was exergonic. 31.2 kcal mol^{-1} and 11.6–16.4 kcal mol^{-1} are released during the formation of **9d** and **12d**, respectively.

On the other hand, the energy profile for the reaction of the CF_3 radical with styrene **1d′** (Fig. 7b, blue color) presented analogous energy barriers for the addition of the radical to the arene (10.5–12.2 kcal mol^{-1}). However, the barrier for the addition to the alkene moiety resulted in significantly smaller values (7.5 kcal mol^{-1}). This difference (3 kcal mol^{-1}) accounts for the selective oxytrifluoromethylations achieved when styrene derivatives are reacted with CF_3 radicals in organic aqueous media.[21] The fate of the trifluoromethylsulfonyl (CF_3SO_2) radical that is initially formed and triggers the reaction mechanism (Fig. 5) was also modelled at the same level of theory. Notably, the calculations also predicted rapid decomposition of the radical with extrusion of SO_2, with an energy barrier of only 5.9 kcal mol^{-1}. This low barrier explained that only minor amounts of products containing the trifluoromethylsulfonyl moiety, *via* trapping of this radical, were observed experimentally.

Conclusions

In summary, the present work provides a detailed experimental and theoretical study on the reactivity of electrochemically generated CF_3 radicals with aryl alkynes in the presence of water. The radicals were generated by anodic oxidation of CF_3SO_2Na in an undivided cell. Similar reactivity toward radicals of the alkyne and arene moieties led to two major reaction pathways: trifluoromethylation of the aromatic ring and oxytrifluoromethylation of the alkyne. The oxytrifluoromethylation process produced a 2-trifluoromethyl enol that upon tautomerization resulted in the formation of an α-trifluoromethyl ketone. The effect on the product distribution of several reaction parameters was evaluated. Formation of α-trifluoromethyl ketones was favored in most cases, except when THF or MeTHF was used as the solvent. Several aryl alkynes decorated with electron-withdrawing and donating groups were tested. The reaction performed well in all cases, although it always led to mixtures of products from the two competing pathways. A computational study of the radical additions to the arene and alkyne, leading to the two competing mechanisms, was carried out at the M06-2X/6-311+G(d,p) level. The analogous energy barriers calculated for all the radical additions successfully explained the selectivity observed experimentally.

Experimental section

General

^{1}H NMR spectra were recorded on a 300 MHz instrument. ^{13}C NMR and ^{19}F NMR spectra were recorded on the same instrument at 75 MHz and 282 MHz, respectively. Routine ^{19}F NMR monitoring was carried out in a Magritek Spinsolve 43 benchtop NMR instrument. Chemical shifts (δ) are expressed in ppm downfield from TMS as the internal standard. The letters s, d, t, q, and m are used to indicate singlet, doublet, triplet, quadruplet, and multiplet, respectively. GC-FID analysis was performed on a ThermoFisher Focus GC with a flame ionization detector, using a TR-5MS column (30 m × 0.25 mm ID × 0.25 μm) and helium as the carrier gas (1 mL min^{-1} constant flow). The injector temperature was set to 280 °C. After 1 min at 50 °C, the temperature was increased by 25 °C min^{-1} to 300 °C and kept constant at 300 °C for 4 min. The detector gases used for flame ionization were hydrogen and synthetic air (5.0 quality). GC-MS spectra were recorded using a ThermoFisher Focus GC coupled with a DSQ II (EI, 70 eV). A TR-5MS column (30 m × 0.25 mm × 0.25 μm) was used, with helium as the carrier gas (1 mL min^{-1} constant flow). The injector temperature was set to 280 °C. After 1 min at 50 °C, the temperature was increased by 25 °C min^{-1} to 300 °C and kept at 300 °C for 3 min. Analytical HPLC analysis was carried out on a C18 reversed-phase (RP) analytical column (150 × 4.6 mm, particle size 5 mm) at 37 °C by using mobile phases A [water/acetonitrile 90 : 10 (v/v) + 0.1% TFA] and B (acetonitrile + 0.1% TFA) at a flow rate of 1.5 mL min^{-1}. The following gradient was applied: a linear increase from solution 30% B to 100% B in 8 min, and hold at 100% solution B for 2 min. Flash chromatography purifications were carried out on an automated flash chromatography system using cartridges packed with KP-SIL, 60 Å (32–63 μm particle size). Sodium trifluoromethanesulfinate (Code: 743232, Lot: BCBX4470), tetrabutylammonium tetrafluoroborate (Code: 217964, Lot: BCBV1430), tetraethylammonium tetrafluoroborate (Code: 242144, Lot: BCBV4670) and lithium perchlorate (Code: 634565, Lot: 0000011388) were purchased from Aldrich. All other chemicals were obtained from standard commercial vendors and were used without any further purification. Electrochemical reactions and cyclic voltammetry experiments were carried out in an IKA ElectraSyn 2.0.

Computational details

All calculations were carried out with the Gaussian 09 package.[24] The M06-2X density functional method[22] in conjunction with the 6-311+G(d,p) basis set was selected for all the geometry optimizations and frequency analysis. The geometries were optimized with the inclusion of solvation effects. For this purpose, the SMD solvation method[23] was employed using acetone as the solvent. Frequency calculations at 298.15 K on all stationary points were carried out at the same level of theory as the geometry optimizations to ascertain the nature of the stationary points. Ground and transition states were characterized by none and one imaginary frequency,

Open Access Article. Published on 12 March 2019. Downloaded on 2/11/2026 1:35:32 PM.
This article is licensed under a Creative Commons Attribution-NonCommercial 3.0 Unported Licence.

respectively. All of the presented relative energies are free energies at 298.15 K.

Experimental procedure for the electrochemical transformation of aromatic alkynes on the preparative scale

All reactions were carried out in an IKA ElectraSyn 2.0 using an IKA Graphite SK-50 anode and an IKA Stainless steel cathode. In a 5 mL IKA ElectraSyn vial, equipped with a stir bar, 0.5 mmol electrolyte (tetraethylammonium tetrafluoroborate, Et_4NBF_4), 1.2 mmol $NaSO_2CF_3$ and 1 mmol alkyne were mixed with 5 mL acetone and 250 μL water. After assembly of the electrochemical cell, the reaction mixtures were purged with N_2 for five minutes prior to switching on electricity to ensure an oxygen- and CO_2-free atmosphere. The instrument was operated in a constant current mode (15 mA) and 2.2 F mol^{-1} of charge were passed. After completion of the reaction, the crude product mixture was concentrated under reduced pressure and the residue was purified by flash column chromatography using petroleum ether/ethyl acetate as the eluent.

1-(4-*tert*-Butyl)phenyl-3,3,3-trifluoropropan-1-one (2a). 86 mg (36%); yellow oil; ^{1}H NMR (300 MHz, $CDCl_3$) δ 7.88 (d, J = 8.1 Hz, 2H), 7.52 (d, J = 8.1 Hz, 2H), 3.77 (q, J = 10.0 Hz, 2H), 1.35 (s, 9H). ^{13}C NMR (75 MHz, $CDCl_3$) δ 189.4, 158.3, 133.4 (d, J = 1.8 Hz), 128.4, 126.0, 124.0 (q, J = 244.5 Hz), 42.1 (q, J = 28.1 Hz), 35.4, 31.1. ^{19}F NMR (282 MHz, $CDCl_3$) δ −61.98 (t, J = 10.1 Hz). MS-EI: m/z 229 (75%), 201 (24%), 161 (30%), 110 (100%).

3,3,3-Trifluoro-1-(4-fluorophenyl)propan-1-one (2b). 35 mg (19%); yellow oil; ^{1}H NMR (300 MHz, $CDCl_3$) δ 8.02–7.92 (m, 2H), 7.25–7.11 (m, 2H), 3.77 (q, J = 9.9 Hz, 2H). ^{13}C NMR (75 MHz, $CDCl_3$) δ 188.3, 168.2, 164.8, 132.4, 131.4, 131.2, 124.0 (q, J = 277.1 Hz), 116.5, 116.2, 42.3 (q, J = 28.3 Hz). ^{19}F NMR (282 MHz, $CDCl_3$) δ −62.03 (t, J = 10.0 Hz, 3F), −102.86 (m, 1F). MS-EI: m/z 206 (6%), 123 (100%), 95 (76%).

4-(3,3,3-Trifluoropropanoyl)benzaldehyde (2c). 23 mg (11%); yellow oil; ^{1}H NMR (300 MHz, $CDCl_3$) δ 10.13 (s, 1H), 8.09 (d, J = 8.4 Hz, 2H), 8.02 (d, J = 8.4 Hz, 2H), 3.85 (q, J = 9.8 Hz, 2H). ^{13}C NMR (75 MHz, $CDCl_3$) δ 191.4, 189.3, 139.8, 130.1, 129.1, 123.8 (q, J = 276.0 Hz), 42.7 (q, J = 28.6 Hz). ^{19}F NMR (282 MHz, $CDCl_3$) δ −62.01 (t, J = 9.8 Hz). MS-EI: m/z 216 (7%), 133 (80%), 105 (35%).

3,3,3-Trifluoro-1-phenylpropan-1-one (2d). 47 mg (27%); yellow oil; ^{1}H NMR (300 MHz, $CDCl_3$) δ 7.99–7.91 (m, 2H), 7.68–7.60 (m, 1H), 7.55–7.48 (m, 2H), 3.80 (q, J = 10.0 Hz, 2H). ^{13}C NMR (75 MHz, $CDCl_3$) δ 189.8, 135.9, 134.4, 129.1, 128.5, 124.1 (q, J = 277.0 Hz), 42.2 (q, J = 28.2 Hz). ^{19}F NMR (282 MHz, $CDCl_3$) δ −62.04 (t, J = 9.9 Hz). MS-EI: m/z 188 (8%), 105 (100%), 77 (86%).

1-(4-Bromophenyl)-3,3,3-trifluoropropan-1-one (2f). 26 mg (10%); yellow oil; ^{1}H NMR (300 MHz, $CDCl_3$) δ 7.85–7.75 (m, 2H), 7.70–7.61 (m, 2H), 3.76 (q, J = 9.9 Hz, 2H). ^{13}C NMR (75 MHz, $CDCl_3$) δ 188.9, 134.6, 132.5, 130.0, 129.8, 123.9 (q, J = 277.1 Hz), 42.3 (q, J = 28.5 Hz). ^{19}F NMR (282 MHz, $CDCl_3$) δ −61.99 (t, J = 9.9 Hz). MS-EI: m/z 185 (93%), 183 (100%), 157 (64%), 155 (26%), 76 (98%), 74 (81%).

3,3,3-Trifluoro-1-(*o*-tolyl)propan-1-one (2g). 54 mg (29%); yellow oil; ^{1}H NMR (300 MHz, $CDCl_3$) δ 7.65–7.59 (m, 1H), 7.42–7.47 (m, 1H), 7.31 (t, J = 7.3 Hz, 2H), 3.75 (q, J = 10.1 Hz, 2H), 2.54 (s, 3H). ^{13}C NMR (75 MHz, $CDCl_3$) δ 192.9 (d, J = 2.4 Hz), 139.7, 136.0, 132.7, 132.6, 129.6, 129.1, 126.2, 124.1 (q, J = 277.1 Hz), 44.5 (q, J = 27.7 Hz), 21.7. ^{19}F NMR (282 MHz, $CDCl_3$) δ −62.09 (t, J = 10.0 Hz). MS-EI: m/z 202 (10%), 119 (74%), 91 (100%).

3,3,3-Trifluoro-1-(*p*-tolyl)propan-1-one (2h). 66 mg (35%); yellow oil; ^{1}H NMR (300 MHz, $CDCl_3$) δ 7.83 (d, J = 8.3 Hz, 2H), 7.30 (d, J = 8.3 Hz, 2H), 3.77 (q, J = 10.0 Hz, 2H), 2.43 (s, 3H). ^{13}C NMR (75 MHz, $CDCl_3$) δ 189.4 (d, J = 2.4 Hz), 145.5, 133.5 (d, J = 1.6 Hz), 129.8, 128.6, 124.2 (q, J = 275.3 Hz), 42.12 (q, J = 28.1 Hz), 21.9. ^{19}F NMR (282 MHz, $CDCl_3$) δ −62.02 (t, J = 10.0 Hz). MS-EI: m/z 202 (11%), 119 (99%), 91 (100%).

3,3,3-Trifluoro-1-(thiophen-2-yl)propan-1-one (2i). 47 mg (27%); yellow oil; ^{1}H NMR (300 MHz, $CDCl_3$) δ 7.76–7.72 (m, 2H), 7.18 (dd, J = 4.9, 3.9 Hz, 1H), 3.71 (q, J = 10.1 Hz, 2H). ^{13}C NMR (75 MHz, $CDCl_3$) δ 182.3 (d, J = 2.8 Hz), 143.3 (d, J = 2.0 Hz), 135.9, 133.6, 128.6, 123.8 (q, J = 277.3 Hz), 43.2 (q, J = 28.7 Hz). ^{19}F NMR (282 MHz, $CDCl_3$) δ −61.94 (t, J = 10.1 Hz). MS-EI: m/z 194 (9%), 111 (100%), 83 (23%).

Conflicts of interest

There are no conflicts to declare.

Acknowledgements

The CC FLOW Project (Austrian Research Promotion Agency FFG No. 862766) is funded through the Austrian COMET Program by the Austrian Federal Ministry of Transport, Innovation and Technology (BMVIT), the Austrian Federal Ministry of Science, Research and Economy (BMWFW), and by the State of Styria (Styrian Funding Agency SFG).

References

1 (*a*) J.-P. Bégué and D. Bonnet-Delphon, *Bioorganic and Medicinal Chemistry of Fluorine*, John Wiley & Sons, Hoboken, 2008; (*b*) *Fluorine in Medicinal Chemistry and Chemical Biology*, ed. I. Ojima, Wiley-VCH, Chichester, 2009.

2 (*a*) D. O'Hagan, *Chem. Soc. Rev.*, 2008, **37**, 308–319; (*b*) K. Müller, C. Faeh and F. Diederich, *Science*, 2007, **317**, 1881–1886; (*c*) H.-J. Böhm, D. Banner, S. Bendels, M. Kansy, B. Kuhn, K. Müller, U. Obst-Sander and M. Stahl, *ChemBioChem*, 2004, **5**, 634–643.

3 (*a*) H.-X. Song, Q.-Y. Han, C.-L. Zhao and C.-P. Zhang, *Green Chem.*, 2018, **20**, 1662–1731; (*b*) C. Alonso, E. Martínez de Marigorta, G. Rubiales and F. Palacios, *Chem. Rev.*, 2015, **115**, 1847–1935.

4 For selected recent reviews on trifluoromethylation chemistry see: (*a*) G.-b. Li, C. Zhang, C. Song and Y.-d. Ma, *Beilstein J. Org. Chem.*, 2018, **14**, 155–181; (*b*) E. H. Oh, H. J. Kim and S. B. Han, *Synthesis*, 2018, **50**, 3346–3358;

 This journal is © The Royal Society of Chemistry 2019

Open Access Article. Published on 12 March 2019. Downloaded on 2/11/2026 1:35:32 PM.
This article is licensed under a Creative Commons Attribution-NonCommercial 3.0 Unported Licence.

(*c*) W. Wu and Z. Weng, *Synthesis*, 2018, **50**, 1958–1964; (*d*) Q. Lefebvre, *Synlett*, 2017, **28**, 19–23; (*e*) A. Prieto, O. Baudoin, D. Bouyssi and N. Monteiro, *Chem. Commun.*, 2016, **52**, 869–881; (*f*) M. Akita and T. Koike, *C. R. Chim.*, 2015, **18**, 742–751; (*g*) P. Gao, X.-R. Song, X.-Y. Liu and Y.-M. Liang, *Chem. – Eur. J.*, 2015, **21**, 7648–7661; (*h*) J. Charpentier, N. Früh and A. Togni, *Chem. Rev.*, 2015, **115**, 650–682.

5 D. A. Nagib and D. W. C. MacMillan, *Nature*, 2011, **480**, 224–228.

6 (*a*) Y. Itoh and K. Mikami, *Org. Lett.*, 2005, **7**, 4883–4885; (*b*) P. V. Pham, D. A. Nagib and D. W. C. MacMillan, *Angew. Chem., Int. Ed.*, 2011, **50**, 6119–6122.

7 (*a*) Y.-b. Wu, G.-p. Lu, T. Yuan, Z.-b. Xu, L. Wan and C. Cai, *Chem. Commun.*, 2016, **52**, 13668–13670; (*b*) M. Oishi, H. Kondo and H. Amii, *Chem. Commun.*, 2009, 1909–1911.

8 H. Guyon, H. Chachignon and D. Cahard, *Beilstein J. Org. Chem.*, 2017, **13**, 2764–2799.

9 N. Shibata, A. Matsnev and D. Cahard, *Beilstein J. Org. Chem.*, 2010, **6**(65), DOI: 10.3762/bjoc.6.65.

10 K. Sato, T. Yuki, R. Yamaguchi, T. Hamano, A. Tarui, M. Omote, I. Kumadaki and A. Ando, *J. Org. Chem.*, 2009, **74**, 3815–3819.

11 (*a*) L. Li, Q.-Y. Chen and Y. Guo, *J. Org. Chem.*, 2014, **79**, 5145–5152; (*b*) K. Mikami, Y. Tomita, Y. Ichikawa, K. Amikura and Y. Itoh, *Org. Lett.*, 2006, **8**, 4671–4673.

12 (*a*) P. V. Pham, D. A. Nagib and D. W. C. MacMillan, *Angew. Chem., Int. Ed.*, 2011, **50**, 6119–6122; (*b*) D. Cantillo, O. de Frutos, J. A. Rincón, C. Mateos and C. O. Kappe, *Org. Lett.*, 2014, **16**, 896–899.

13 T. Kitazume and N. Ishikawa, *J. Am. Chem. Soc.*, 1985, **107**, 5186–5191.

14 For selected examples, see: (*a*) Y. Yang, Y. Liu, Y. Jiang, Y. Zhang and D. A. Vicic, *J. Org. Chem.*, 2015, **80**, 6639–6648; (*b*) E. Yamaguchi, Y. Kamito, K. Matsuo, J. Ishihara and A. Itoh, *Synthesis*, 2018, **50**, 3161–3168; (*c*) Y.-b. Wu, G.-p. Lu, T. Yuan, Z.-b. Xu, L. Wan and C. Cai, *Chem. Commun.*, 2016, **52**, 13668–13670; (*d*) A. Deb, S. Manna, A. Modak, T. Patra, S. Maity and D. Maiti, *Angew. Chem., Int. Ed.*, 2013, **52**, 9747–9750.

15 (*a*) A. Maji, A. Hazra and D. Maiti, *Org. Lett.*, 2014, **16**, 4524–4527; (*b*) Y. R. Malpani, B. K. Biswas, H. S. Han, Y.-S. Jung and S. B. Han, *Org. Lett.*, 2018, **20**, 1693–1697.

16 For recent reviews on the applications of electrochemistry to organic synthesis, see: (*a*) M. Yan, Y. Kawamata and P. S. Baran, *Chem. Rev.*, 2017, **117**, 13230–13319; (*b*) P.-G. Echeverria, D. Delbrayelle, A. Letort, F. Nomertin, M. Perez and L. Petit, *Aldrichimica Acta*, 2018, **51**, 3–19; (*c*) S. R. Waldvogel, A. Wiebe, T. Gieshoff, S. Möhle, E. Rodrigo and M. Zirbes, *Angew. Chem., Int. Ed.*, 2018, **57**, 5594–5619; (*d*) S. R. Waldvogel and B. Janza, *Angew. Chem., Int. Ed.*, 2014, **53**, 7122–7123.

17 E. J. Horn, B. R. Rosen and P. S. Baran, *ACS Cent. Sci.*, 2016, **2**, 302–308.

18 (*a*) R. N. Renaud and P. J. Champagne, *Can. J. Chem.*, 1975, **53**, 529–534; (*b*) K. Arai, K. Watts and T. Wirth, *ChemistryOpen*, 2014, **3**, 23–28.

19 Many applications of electrochemical oxidation of CF_3SO_2Na for trifluoromethylation reactions have been recently reported, a strategy originally described by Langlois: (*a*) B. R. Langlois, E. Laurent and N. Roidot, *Tetrahedron Lett.*, 1991, **32**, 7525–7528; (*b*) J.-B. Tommasino, A. Brondes, M. Médebielle, M. Thomalla, B. R. Langlois and T. Billard, *Synlett*, 2002, 1697–1699.

20 A. G. ÓBrien, A. Maruyama, Y. Inokuma, M. Fujita, P. S. Baran and D. G. Blackmond, *Angew. Chem., Int. Ed.*, 2014, **53**, 11868–11871.

21 W. Jud, C. O. Kappe and D. Cantillo, *Chem. – Eur. J.*, 2018, **24**, 17234–17238.

22 Y. Zhao and D. G. Truhlar, *Theor. Chem. Acc.*, 2008, **120**, 215–241.

23 A. V. Marenich, C. J. Cramer and D. G. Truhlar, *J. Phys. Chem. B*, 2009, **113**, 6378–6396.

24 M. J. Frisch, G. W. Trucks, H. B. Schlegel, G. E. Scuseria, M. A. Robb, J. R. Cheeseman, G. Scalmani, V. Barone, B. Mennucci, G. A. Petersson, H. Nakatsuji, M. Caricato, X. Li, H. P. Hratchian, A. F. Izmaylov, J. Bloino, G. Zheng, J. L. Sonnenberg, M. Hada, M. Ehara, K. Toyota, R. Fukuda, J. Hasegawa, M. Ishida, T. Nakajima, Y. Honda, O. Kitao, H. Nakai, T. Vreven, J. A. Montgomery Jr., J. E. Peralta, F. Ogliaro, M. Bearpark, J. J. Heyd, E. Brothers, K. N. Kudin, V. N. Staroverov, R. Kobayashi, J. Normand, K. Raghavachari, A. Rendell, J. C. Burant, S. S. Iyengar, J. Tomasi, M. Cossi, N. Rega, J. M. Millam, M. Klene, J. E. Knox, J. B. Cross, V. Bakken, C. Adamo, J. Jaramillo, R. Gomperts, R. E. Stratmann, O. Yazyev, A. J. Austin, R. Cammi, C. Pomelli, J. W. Ochterski, R. L. Martin, K. Morokuma, V. G. Zakrzewski, G. A. Voth, P. Salvador, J. J. Dannenberg, S. Dapprich, A. D. Daniels, Ö. Farkas, J. B. Foresman, J. V. Ortiz, J. Cioslowski and D. J. Fox, *Gaussian 09, Revision A.1*, Gaussian, Inc., Wallingford CT, 2009.